Nonlinearity of Pancharatnam's geometric phase in polarizing interferometers

Bernhard Hils, Wolfgang Dultz,* and Werner Martienssen
Physikalisches Institut der Universität Frankfurt, Robert-Mayer-Straße 2-4, 60054 Frankfurt-am-Main, Germany
(Received 10 December 1998)

Earlier investigations show a time-variable nonlinear shift of the fringe pattern in a polarizing interferometer while rotating a polarizer at the exit. This effect was identified as Pancharatnam's geometrical phase and proposed for applications in interferometry and fast optical switching devices. A heterodyne analysis attributes moving fringes to a frequency difference between the interfering beams; thus changing fringe velocities point to a dynamic frequency development within the period of the uniformly rotating analyzer. This explanation offends the intuition and we undertake an experimental and theoretical investigation of the effect to solve the paradox. We determine, e.g., the complete frequency and mode spectrum of an arbitrary state of polarization P_0 behind a rotating linear analyzer and behind a rotating arbitrary linear birefringent plate. We find that, in spite of a fast changing phase in the interferometer, no other (higher) frequency components appear in the spectral distribution of the intensity at the exit than the double of the rotary frequency of the analyzer: phase nonlinearities are compensated for by intensity changes. Only a phase-sensitive detector like an array of photodetectors is able to observe the nonlinearity of Pancharatnam's geometrical phase. A single detector only finds a sinusoidal intensity variation. Our insight into these relations leads us to two new applications of Pancharatnam's phase: supersensitivity of a polarizing double beam interferometer with a video camera acting as a phase detector and external tuning of a Fizeau interferometer. [S1063-651X(99)09308-3]

PACS number(s): 42.25.Ja, 07.60.Ly, 03.65.Bz

I. INTRODUCTION

The nonlinear dependence of an observable of a physical system with respect to one of the system parameters may often find useful applications in measuring techniques. A system in which small changes in the input generate large output changes acts as an amplifier within certain limits. The amplification of the changes of the phase of light, e.g., would be advantageous since it could be used to increase the speed and sensitivity of interferometric switches in optical communications and reduce their driving power. Not all nonlinearities in optics depend on materials with a nonlinear optical susceptibility where the light intensity is the initiating quantity. In this paper we wish to investigate the extremely nonlinear behavior of the optical phase changes in polarizing interferometers due to one of the optical Berry phases, namely Pancharatnam's phase, which appears without the use of any nonlinear materials.

Pancharatnam's phase γ is introduced by an analyzer P between the interfering light beams at the exit of a polarizing interferometer. In 1956, Pancharatnam [1] showed that two coherent light beams with the states of polarizations P_1 and P_2 gain a phase difference γ, if they pass an analyzer P. γ only depends on the polarizations P_1, P_2, and P and is given by Pancharatnam's theorem:

$$\gamma = -\tfrac{1}{2}\Omega(P_1,P_2,P). \tag{1.1}$$

$\Omega(P_1,P_2,P)$ is the area of the spherical triangle P_1,P_2,P (the spherical excess) on the Poincaré sphere. Surprisingly, Pancharatnam's phase does not depend on the wavelength λ nor the optical path length ln like the dynamical phase $\delta = 2\pi(ln/\lambda)$ of light, n being the refractive index. It is achromatic, and a pure phenomenon of linear optics. Other interesting properties of Pancharatnam's phase are its unboundedness [2] and its unlimited additivity to the dynamical phase down into the quantum regime [3]. A number of interesting applications of these characteristic features have been found in optical switching [4,5], endless phase control [2], remote interferometer tuning [6], and novel optical components [7].

From the physical point of view, Pancharatnam's phase is a member of the family of the Berry phases or geometric phases [8–10]. A geometric phase describes the phase gain of the quantum state of a particle due to adiabatic changes, which turn the system around a closed path in parameter space back to its original state. This phase gain can only be measured with the help of an interference experiment: a coherent particle beam is split, both parts are led on different pathways to the same point in parameter space, and then their phase difference is determined interferometrically. Already in his first paper [11] on this subject, Berry mentioned the photon as a possible candidate for his theory and proposed an experiment.

Up to now, Pancharatnam's phase has drawn the largest attention among the optical geometric phases. In this study we want to investigate an extraordinary *nonlinearity* of Pancharatnam's phase. It was shown that, with the help of Pancharatnam's phase, the tuning of a polarizing two-beam interferometer may vary nonlinearly, if the polarizations P_1,P_2 of the beams are located close to each other on the Poincaré sphere [12,13]. In this case, a changing analyzer P at the exit of the polarization-coded interferometer generates moving fringes with a wide range of shift velocities depending on the actual analyzer orientation. A shift velocity of interference fringes usually corresponds to a frequency difference between the interfering beams. We are now confronted with the puzzling conclusion that a changing analyzer seems to introduce frequency sidebands into the output

*Present address: Deutsche Telekom AG, Technologiezentrum, 64276 Darmstadt, Germany.

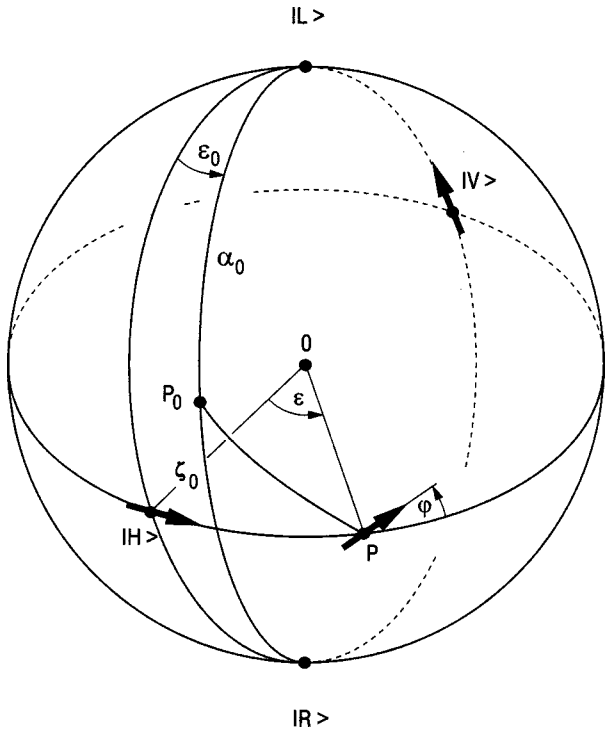

FIG. 1. Definition of the state of polarization P_0 resolved by an analyzer P on the Poincaré sphere.

beam of the interferometer, which not only depend on the alteration of the analyzer but also and predominantly on the polarization coding of the interferometer.

In this paper we wish to show that this is not the case. A rotating linear analyzer which introduces Pancharatnam's phase generates frequency side bands of twice the rotation frequency in spite of the fact that the interference fringes move very slowly or very fast. An experiment with a rotating linear analyzer confirms this result. But we also show that the nonlinear phase change exists and can have useful applications in optical measuring technology for telecommunications.

II. THEORY

The usual interferometric measurement uses a single photodetector in the interference field at the exit of the instrument. The light intensity at the detector (the fringe pattern) is monitored while the interferometer is tuned by changing the optical path length or the wavelength of light. In both cases, the phase difference between the interfering light beams is changed. In our case, the tuning parameter is the state of polarization of the analyzer P: P introduces Pancharatnam's phase difference γ into the interferometer; the interferometer is tuned by changing the state of polarization P.

We consider the polarization P_0 at a certain point of the interference field in front of the analyzer P; after passing the analyzer P, P_0 is projected onto P and we call it P_1.

To determine the frequency component of P_1, we use a spinor-type formalism of orthogonal polarization eigenfunctions on the Poincaré sphere [9]. The relations are illustrated in Fig. 1. An arbitrary state of polarization P_0 is defined by its angular coordinates ε_0 and ζ_0. Two different pairs of orthogonal basis functions are used: the linear basis H/V and the circular basis L/R,

$$H=\begin{pmatrix}1\\0\end{pmatrix}, \quad V=\begin{pmatrix}0\\1\end{pmatrix}, \tag{2.1}$$

$$L=\frac{1}{\sqrt{2}}\begin{pmatrix}1\\-i\end{pmatrix}, \quad R=\frac{1}{\sqrt{2}}\begin{pmatrix}1\\i\end{pmatrix}. \tag{2.2}$$

Since we want to study the time dependence of a polarized light wave of frequency ω, we introduce the phase factor $\exp(i\omega t)$ to obtain the eigenfunctions: $|H\rangle = H\exp(i\omega t)$, $|L\rangle = L\exp(i\omega t)$, etc.

An arbitrary light wave of polarization P_0 is given by

$$|P_0\rangle = \cos\frac{\alpha_0}{2}\exp\left(i\frac{\varepsilon_0}{2}\right)|L\rangle + \sin\frac{\alpha_0}{2}\exp\left(-i\frac{\varepsilon_0}{2}\right)|R\rangle \tag{2.3}$$

in the circular basis. A linear analyzer P which rotates at a frequency ω_0 in the positive sense and transmits the light wave $|P\rangle$ while absorbing the orthogonal component $|\overline{P}\rangle$ moves from west to east around the equator of the Poincaré sphere with the angular frequency:

$$\frac{d\varepsilon}{dt}=2\frac{d\varphi}{dt}=2\omega_0, \tag{2.4}$$

$$|P\rangle = \frac{1}{\sqrt{2}}\exp(i\omega_0 t)|L\rangle + \frac{1}{\sqrt{2}}\exp(-i\omega_0 t)|R\rangle, \tag{2.5}$$

$$|\overline{P}\rangle = \frac{1}{\sqrt{2}}\exp(i\omega_0 t)|L\rangle - \frac{1}{\sqrt{2}}\exp(-i\omega_0 t)|R\rangle. \tag{2.6}$$

We assume the nonrelativistic case $\omega_0 \ll \omega$. To obtain the frequency components of an arbitrary light wave of polarization P_0 and frequency ω after passing the rotating linear analyzer P, we use the projection operator $|P\rangle\langle P|$ and apply it to $|P_0\rangle$,

$$\begin{aligned}|P_1\rangle &= |P\rangle\langle P|P_0\rangle \\ &= \frac{1}{2}\Bigg[\cos\tfrac{1}{2}\alpha_0\exp\left(i\frac{\varepsilon_0}{2}\right)|L\rangle \\ &\quad + \cos\tfrac{1}{2}\alpha_0\exp\left(i\frac{\varepsilon_0}{2}\right)\exp(-i2\omega_0 t)|R\rangle \\ &\quad + \sin\tfrac{1}{2}\alpha_0\exp\left(-i\frac{\varepsilon_0}{2}\right)\exp(i2\omega_0 t)|L\rangle \\ &\quad + \sin\tfrac{1}{2}\alpha_0\exp\left(-i\frac{\varepsilon_0}{2}\right)|R\rangle\Bigg].\end{aligned} \tag{2.7}$$

Behind the rotating linear analyzer $|P_1\rangle$ contains four different frequency components (2.7); two components of polarization L and R, which are not shifted in frequency, one component of polarization R is shifted downward $2\omega_0$, and one component of polarization L is shifted upward $2\omega_0$. This is valid for an analyzer P which rotates in the positive sense (west to east in Fig. 1). We define right (left) circular polarized light with an electric field vector on a right- (left-)

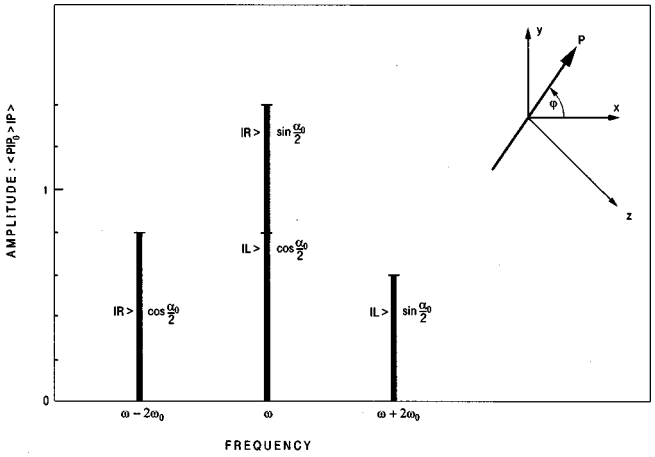

FIG. 2. Amplitude and frequency of the different light modes if the state of polarization P_0 (α_0) passes a rotating linear analyzer P at a frequency of rotation of ω_0.

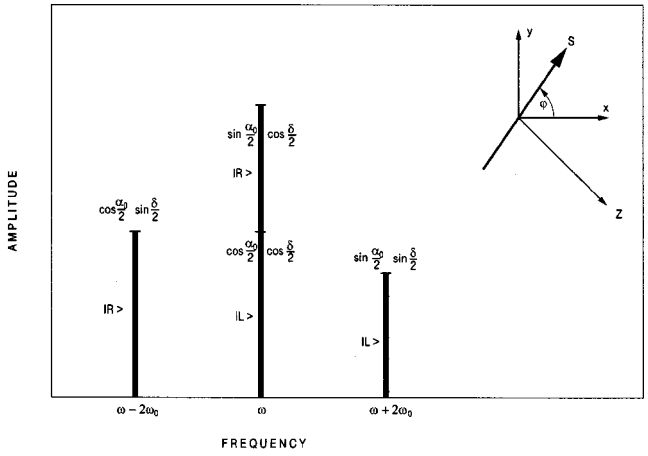

FIG. 3. Amplitude and frequency of the different light modes if the state of polarization P_0 (α_0) passes a rotating linear birefringent plate of retardation angle δ at a frequency of rotation of ω_0.

handed screw (traditional view). For a polarizer which rotates in the opposite sense, the components shifted downward and upward exchange their state of polarization and amplitudes. Figure 2 shows this as a histogram for the amplitudes of the different components of the light wave behind the rotating analyzer. Our result is consistent with earlier work [14].

The projection operator formalism can also be used to calculate the frequency components of $|P_0\rangle$ after a rotating plate of linear birefringence with fast axis P and slow axis $\overline{P}$. In this case the fast and the slow components add up behind the rotating plate with a phase difference δ which describes the retardation in the plate:

$$|P_1\rangle=\langle P|P_0\rangle\exp\left(i\frac{\delta}{2}\right)|P\rangle+\langle\overline{P}|P_0\rangle\exp\left(-i\frac{\delta}{2}\right)|\overline{P}\rangle. \tag{2.8}$$

With Eqs. (2.3), (2.5), and (2.6) we find

$$\begin{aligned}|P_1\rangle=&\cos\frac{\alpha_0}{2}\cos\frac{\delta}{2}\exp\left(i\frac{\varepsilon_0}{2}\right)|L\rangle\\&+i\cos\frac{\alpha_0}{2}\sin\frac{\delta}{2}\exp\left(i\frac{\varepsilon_0}{2}\right)\exp(-i2\omega_0t)|R\rangle\\&+i\sin\frac{\alpha_0}{2}\sin\frac{\delta}{2}\exp\left(-i\frac{\varepsilon_0}{2}\right)\exp(i2\omega_0t)|L\rangle\\&+\sin\frac{\alpha_0}{2}\cos\frac{\delta}{2}\exp\left(-i\frac{\varepsilon_0}{2}\right)|R\rangle.\end{aligned} \tag{2.9}$$

Figure 3 shows the amplitudes of the different frequency components for a linear birefringent plate rotating in the positive sense. Again the polarizations and amplitudes of the components shifted downward and upward are exchanged for a plate rotating in the negative sense. Well known examples are the rotating λ/2 plate with $|P_0\rangle=|L\rangle$ or $|R\rangle$ ($\alpha_0=0,\pi$) in which case only one downshifted or upshifted component remains. If linear polarized light passes a rotating λ/2 plate ($\delta=\pi$, $\alpha_0=\pi/2$), only an upshifted and a downshifted component of opposite circular polarization appear; there are no components unshifted in frequency. For a rotating plate of elliptical birefringence, Eqs. (2.5) and (2.6) have to be extended to express the location of the general state of polarization P and $\overline{P}$ on the Poincaré sphere in the same way as in Eq. (2.3). Since elliptical retardation plates are not common, this case is not very practical.

In case a polarizing interferometer is tuned by Pancharatnam's phase using a rotating linear polarizer, a single detector at the exit only monitors intensity changes with the frequency component $2\omega_0$ (2.7). This is also valid for multiple beam interferometers since the polarization P_0 at the exit of the instrument may be a sum of any number of coherent light beams.

This result seems to be contradictory to the obviously nonlinear shift of Pancharatnam's phase between two coherent light beams of intensity I_1,I_2 and polarization P_1,P_2 behind a rotating linear analyzer P [13]. The interference field I in this case is given by [1] and [15]:

$$I=I_1\cos^2\frac{\alpha}{2}+I_2\cos^2\frac{\beta}{2}+2\sqrt{I_1I_2}\cos\frac{\alpha}{2}\cos\frac{\beta}{2}\cos(\delta+\gamma). \tag{2.10}$$

α and β are the angular distances of P_1 and P_2 from the analyzer P on the Poincaré sphere and δ is the dynamical phase difference between the two beams. Pancharatnam's phase γ can be determined from the spherical excess $\Omega(P_1,P_2,P)$ of the spherical triangle P_1,P_2,P [Eq. (1.1)]. For the symmetric case (Fig. 4), spherical geometry leads to

$$\gamma=\frac{\pi}{2}-\operatorname{arccot}(\sin\eta\cot2\varphi)-\operatorname{arccot}(\cot\eta\sin2\varphi) \tag{2.11}$$

with $\angle(H,P_1)=\angle(H,P_2)=\eta$ and φ being the orientation angle of the analyzer P. γ behaves very nonlinearly with respect to φ when η is small. Inserting Eq. (2.11) into Eq. (2.10), one obtains—after some laborious mathematical operations and with $I_1=I_2$ [16]—the following equation for the intensity of the interference pattern in a single location:

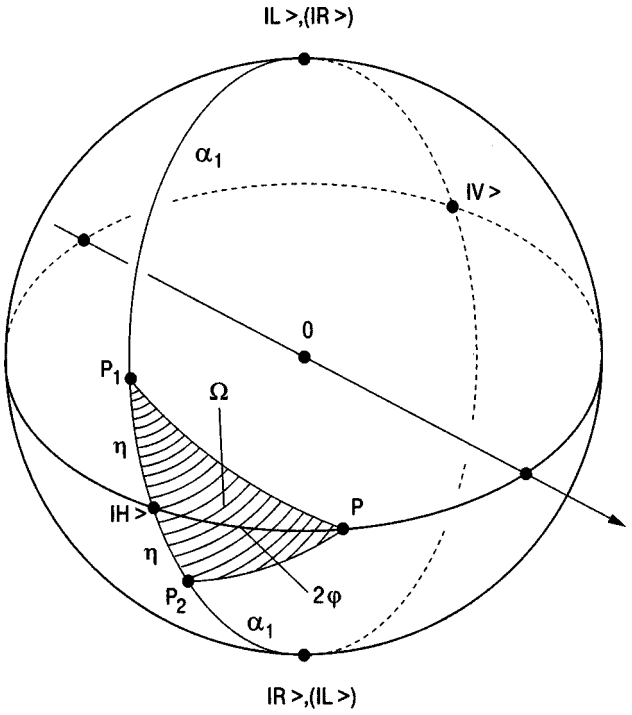

FIG. 4. Poincaré model of two symmetrical states of polarizations P_1, P_2 passing the linear polarizer P.

$$I = I_1(1 + \cos 2\varphi \cos \eta + \cos \delta(\cos 2\varphi + \cos \eta) + \sin \delta \sin \eta \sin 2\varphi). \tag{2.12}$$

The intensity I behind the analyzer P again does not show any local nonlinearities and only contains frequency components of double the rotation frequency $2\omega_0 = 2(d\varphi/dt)$. We have the same result as before that, despite a nonlinear shift of the fringe pattern, a single detector located anywhere in this fringe pattern only monitors the single frequency component $2\omega_0$.

But where is Pancharatnam's phase? Like every phase information, it is a property of the whole interference field. If we cross two coherent light beams of different polarizations P_1 and P_2 (see Fig. 4) we can describe the interference field by a sum of the two polarizations in the same way as in Eq. (2.3):

$$P_1 = \left(\cos\frac{\alpha_1}{2}|L\rangle + \sin\frac{\alpha_1}{2}|R\rangle \right) \exp\left(i\frac{\delta}{2} \right),$$
$$P_2 = \left(\sin\frac{\alpha_1}{2}|L\rangle + \cos\frac{\alpha_1}{2}|R\rangle \right) \exp\left(-i\frac{\delta}{2} \right). \tag{2.13}$$

The two polarizations are assumed to lie symmetrically above and below the equator of the Poincaré sphere on the null meridian ($\varepsilon = 0$) (Fig. 4). δ is the phase difference of the beams at a certain point of the interference field in the crossing region; for plane waves δ is proportional to the transverse spatial coordinate across the beams. We find

$$P_1 + P_2 = \sqrt{2(1 + \sin\alpha_1 \cos\delta)}[\exp(i\psi)|L\rangle + \exp(-i\psi)|R\rangle], \tag{2.14}$$

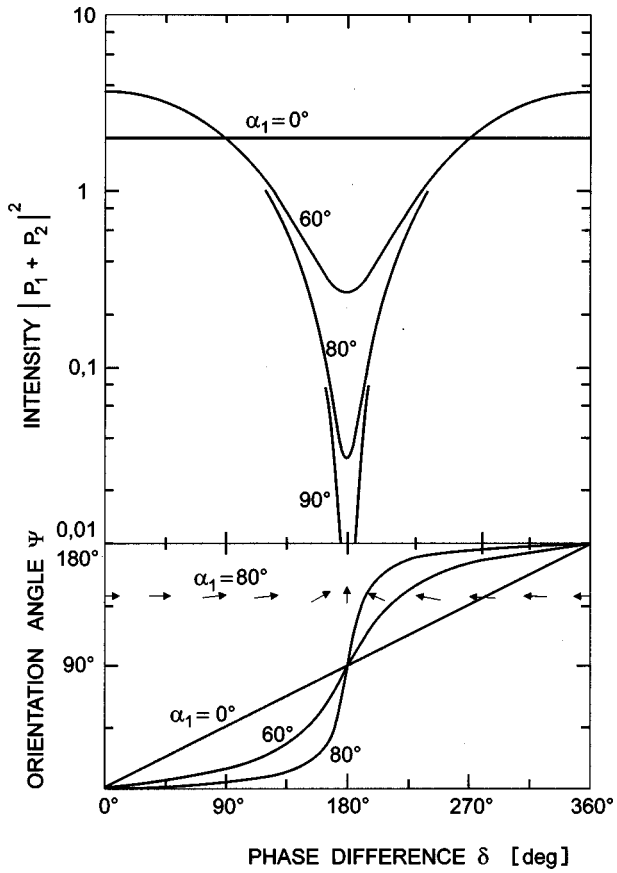

FIG. 5. Intensity and orientation angle of the sum of $P_1 + P_2$ with respect to their initial phase difference δ. α_0 is the distance angle of $P_1 + P_2$ to the poles; see Fig. 4.

$$\psi = \arctan\left(\frac{\cos\frac{\alpha_1}{2} - \sin\frac{\alpha_1}{2}}{\cos\frac{\alpha_1}{2} + \sin\frac{\alpha_1}{2}} \tan\frac{\delta}{2} \right).$$

The orientation angle ψ of the linear polarized light $P_1 + P_2$ depends on δ in a nonlinear way: the two beams generate an interference field with a varying linear polarization angle ψ. Only if they are right and left circular polarized ($\alpha_1 = 0$) is ψ equal to $\delta/2$. A linear analyzer $P(\varphi)$ with orientation angle φ projects the component P with the amplitude $\cos(\varphi - \psi)(P_1 + P_2)$ out of this field and generates the fringe pattern which exhibits Pancharatnam's phase $\gamma(\varphi)$.

Figure 5 (bottom) shows the orientation angle ψ for different polarizations P_1, P_2 in the symmetric case of Fig. 4. The smaller $\angle(P_1, P_2) = 2\eta$, the faster are the changes of ψ with respect to δ near $\delta = \pi$. The small arrows in the lower plot of Fig. 5 demonstrate this for $\alpha_1 = 80°$. In the same region of δ, the intensity $2(1 + \sin\alpha_1 \cos\delta)$ drops according to Eq. (2.14). Figure 5 (top) shows the intensity on a logarithmic scale.

This can be explained with the following qualitative picture. If we add two linear polarizations under a small angle η, we obtain a small transversal component $P_t = P_1 - P_2$ if the interference is destructive ($\delta = \pi$); see Fig. 6. In the constructive case ($\delta = 0$) this transversal component is destructive and disappears. It is this small component P_t being

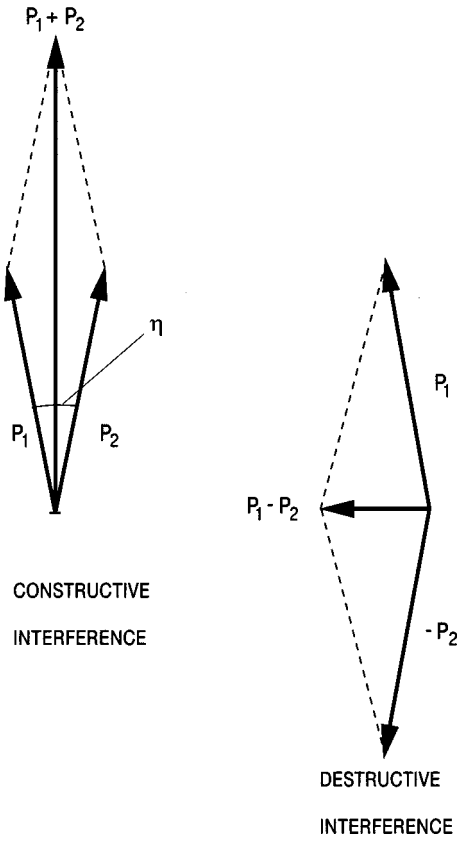

FIG. 6. Qualitative picture describing the phase sensitivity of the small transversal component P_1-P_2.

nearly orthogonal to P_1,P_2 which is the origin of the nonlinearity of Pancharatnam's phase. It changed its state of polarization very fast with δ near $\delta=\pi$. In the case of Fig. 4, it remains linearly polarized but rotates very fast. It is this fast rotation near $\delta=\pi$ and the slow rotation near $\delta=0$ which generate the nonlinear moving fringe pattern behind the rotating analyzer.

III. EXPERIMENT

The Michelson interferometer, which was used to measure Pancharatnam's phase with respect to the orientation angle φ of the rotating analyzer P, is shown in Fig. 7. From the white light of a tungsten lamp, a single line λ_m is selected with the interference filter IF. The light is vertically polarized V and enters the Michelson interferometer through

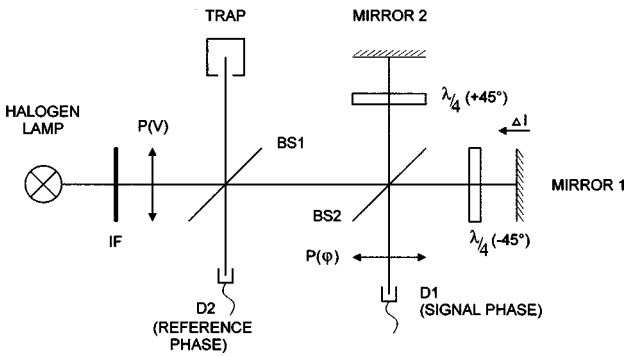

FIG. 7. Experimental setup for measuring the spectral components of P_1+P_2.

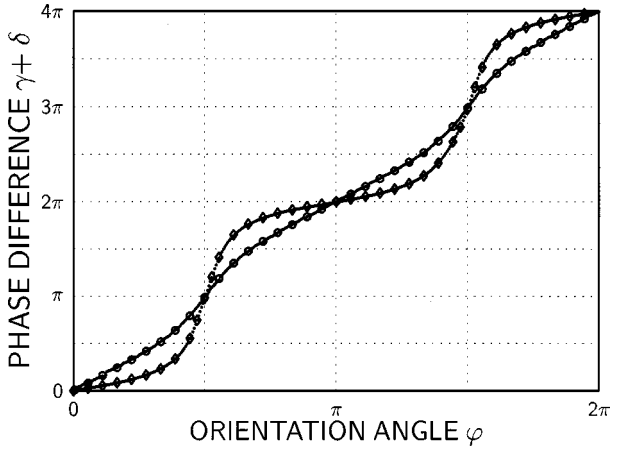

FIG. 8. Pancharatnam's phase measured for two different configurations P_1,P_2. ○○○, at a large angular distance P_1,P_2. ◇◇◇, at a small angular distance P_1,P_2.

the beam splitter cube BS1. In both arms of the interferometer, a $\lambda_R/4$ retardation plate orientated at $\pm 45°$ to V ensures an opposite development of polarization over the north and the south poles of the Poincaré sphere; for $\lambda_m=\lambda_R$ the polarization becomes horizontal H over the north pole in one arm and also horizontal H over the south pole in the other arm. For $\lambda_m\neq\lambda_R$ both arcs over the poles are larger or smaller than π and we obtain the polarizations P_1,P_2 symmetrical to the equator. The rotatable analyzer $P(\varphi)$ introduces Pancharatnam's phase at the exit of the interferometer and the detector $D1$ measures the intensity. To obtain a reference phase, we measure the backreflected π-shifted light from the Michelson interferometer at the detector $D2$. Note that at the second exit of the interferometer at $D2$ there is no analyzer and therefore no geometric phase is introduced. While moving the mirror $M1$, both detectors measure the same dynamical phase but detector $D1$, in addition, measures Pancharatnam's phase. These two signals define an ellipse in a parametric plot from which Pancharatnam's phase γ is extracted.

Figure 8 shows Pancharatnam's phase with respect to the orientation angle φ of the analyzer P for two different configurations of P_1,P_2. Equation (2.11) expresses these measured data points in an excellent way. The smaller the distance $\angle(P_1,P_2)$ on the Poincaré sphere, the more sensitive is the phase to small changes of the orientation angle φ of the analyzer P. The dispersion properties of Pancharatnam's phase $\gamma(\lambda)$ are illustrated in the simulations (Figs. 9 and 10). In Fig. 9 the shade represents the intensity I of the interference of two coherent light beams with the same state of polarization and a phase difference equal to $\delta+\gamma$,

$$I=2I_0\{1+\cos[\delta(\lambda)+\gamma(\lambda)]\},$$

$\delta(\lambda)=2\pi\Delta\ \ln/\lambda$ is the relative phase deviation between the beams, and $\gamma(\lambda)$ represents Pancharatnam's phase according the geometry of Fig. 4. The dispersion is due to the wavelength dependence of the retardation of the $\lambda/4$ plates (633 nm) in our experimental setup (Fig. 7). In Fig. 9 we can see the singular behavior of $\gamma(\lambda)$ at a wavelength of 633 nm, the plot is qualitatively symmetrical to the wavelength of the $\lambda_R/4$ retardation plates (633 nm). The opposite shift of

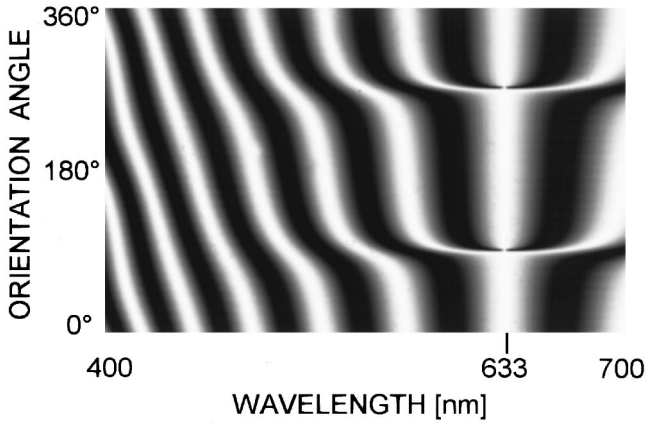

FIG. 9. Intensity pattern of two fictitious light beams of the same state of polarization with a phase difference equal to a constant dynamical phase plus a nonlinear Pancharatnam phase.

fringes with respect to the orientation angle of the analyzer P on the right and the left sides of the symmetry wavelength $\lambda = 633$ nm indicates the opposite sign of the dispersion $\gamma(\lambda)$ in these regions.

The singularities in the intensity at 633 nm disappear when the actual conditions of the experiment are introduced (Fig. 10). Now the two beams have different polarizations P_1, P_2 which depend on λ due to the wavelength dependence of the retardation plates as in the previous case. The analyzer P in the antipodal location on the Poincaré sphere reduces the intensity of $P_1 + P_2$ drastically and smears the strong intensity gradients. The transmission characteristics according to Fig. 10 can be observed while inserting a dispersion prism at the entrance or exit of the interferometer. The number of lines in the spectrum is given by the path difference of the interferometer arms.

The intensity variation at a single detector with respect to the rotating analyzer corresponds to a vertical cut through Fig. 10 at different wavelengths. A single detector only observes a sinusoidal intensity variation in this case. To show this, we rotated the analyzer in Fig. 7 at 50 Hz and determined the frequency components at the exit; see Fig. 11. The intensity $|P_1 + P_2|^2 \cos^2[\psi - \varphi(t)]$ only contains the strong 100 Hz component as expected. If the analyzer rotates in the positive sense, it contains an upshifted (and a downshifted)

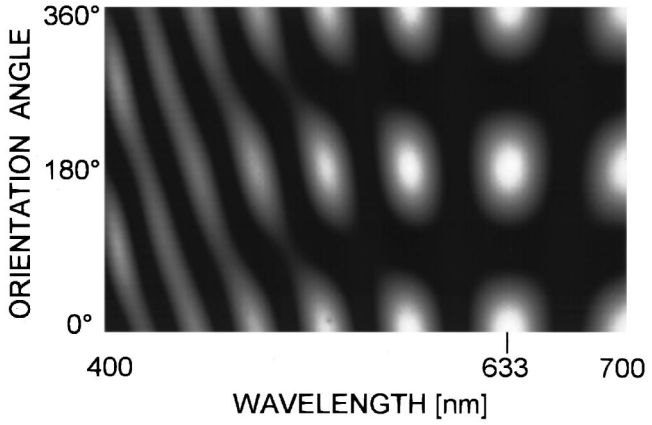

FIG. 10. Intensity pattern of the actual experiment according to Figs. 4 and 7. The singularities of Fig. 9 are smeared.

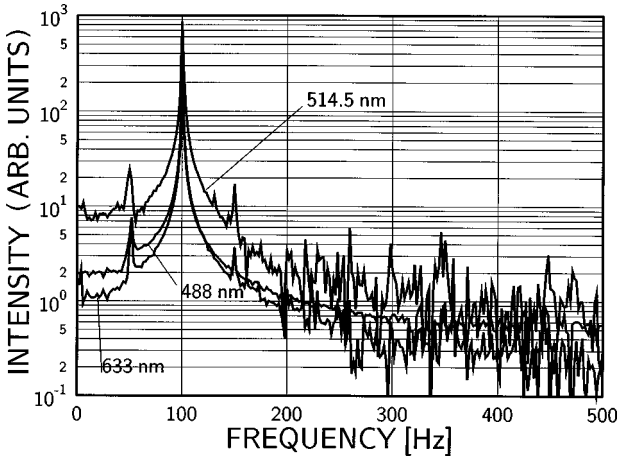

FIG. 11. Frequency spectrum of the intensity at the exit of the Michelson interferometer Fig. 7 behind a linear analyzer P with a rotation frequency of $\omega_0 = 50$ Hz.

component of left (right) circular polarized light and two unshifted components (right and left), according to Fig. 2 ($\alpha_0 = 90°$), all of equal amplitude. Their beat generates the 100 Hz frequency component we are measuring in our experiment, Fig. 11. The small peaks at 50 and 150 Hz are due to transparency variations (dirt) on the analyzer.

IV. APPLICATIONS OF PANCHARATNAM'S PHASE IN INTERFEROMETRY

Pancharatnam's phase has very interesting applications in crystal optics and interferometry [7]. Here we want to discuss two new applications to increase the phase sensitivity of an interferometer.

A. A supersensitive interferometer

The nonlinear shift of Pancharatnam's phase with respect to small changes of an initial phase between two polarized light beams can be used very precisely to measure small refractive index changes in transparent nonbirefringent media or small changes in optical path difference or wavelength. In principle, two coherent light beams with similar but different polarizations P_1, P_2 are superimposed with a continuously varying initial phase difference δ. The developing nonlinear polarization grating, see the small arrows in Fig. 5, of the interference field is overlayed with the analyzer P, which transmits $P \approx \overline{P}_1 \approx \overline{P}_2$, an approximately orthogonal polarization with respect to P_1 and P_2. We obtain fringes which are supersensitive to small changes of δ, P, and/or the wavelength λ. They can be recorded by a video camera and evaluated by a computer.

It is practical to use a Michelson interferometer to implement an instrument for this purpose, Fig. 7. The polarizations P_1, P_2 are generated with retardation plates in each arm and one mirror is tilted to obtain fringes at the exit. The analyzer P is adjusted to the sensitive region as described in the preceding section; the sensitive fringes are observed with a camera. Its dynamic range has to be matched to the fringe intensity, which becomes small in the region of high fringe sensitivity.

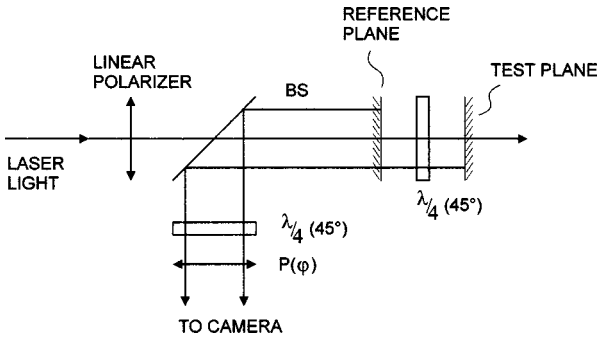

FIG. 12. Fizeau interferometer tuned with Pancharatnam's phase.

B. A Fizeau interferometer with external tuning

Another new interferometric device employed to test optical surfaces uses Pancharatnam's phase to tune a Fizeau interferometer externally, Fig. 12. In this case, the polarizations P_1, P_2 of the polarizing interferometer are orthogonal (right- and left-circular polarized). The analyzer P is a rotatable linear polarizer.

Linearly polarized light emitted by a coherent light source is partially reflected from the reference surface (reference beam); most of the light is transmitted and again partially reflected from the test surface (measurement beam). A retardation plate rotates the state of polarization of the measurement beam 90°. A beamsplitter decouples the two beams; they are changed into right- and left-circular polarization with a second retardation plate at the exit and analyzed with the analyzer P, which introduces Pancharatnam's phase difference γ between the two beams. Since the beams are orthogonally circular polarized, γ depends linearly on the orientation angle φ of the linear analyzer P. Again one of the surfaces is tilted and the fringe pattern is observed with a video camera.

This modified Fizeau interferometer is tuned only by rotating an analyzer P at the exit of the interferometer. The fringes can be shifted to any location in the interference plane without the need for mechanically tuning the length of the cavity. The interference pattern is evaluated by a computer. This increases the precision of the measurement considerably, since the test—and reference surfaces which may be large and heavy—need not be moved at all for tuning. The high sensitive tuning using the nonlinear behavior of Pancharatnam's phase can be easily introduced by orientating the linear polarization at the entrance at $\sim 45°$ and by replacing the linear analyzer P at the exit by an elliptical analyzer.

It is a great advantage with respect to mechanical stability if an interferometer can be tuned externally. Another advantage of Pancharatnam's phase is the fact that there is no need at all to separate the interfering light beams spatially. The beams can have the same path after they are polarization coded, since the tuning is done by the analyzer P which is transmitted by both of them.

V. CONCLUSIONS

At least four intensity measurements are required to obtain the phase difference between two light beams unambiguously. This is usually done with the eight-port detection device [17], which measures simultaneously four superpositions of the two beams with four definite phase differences at a time. We determine Pancharatnam's phase with a four-port device and a much larger number of measurements: the transmitted and the reflected intensity of a Michelson interferometer is measured while one of the mirrors moves and introduces many definite phases at many different times. A simpler way of measuring phases uses the continuous phase differences over an interference field of two inclined light beams. The whole field is recorded by a video camera and evaluated by a computer.

The important question of how the nonlinearity of Pancharatnam's phase can be applied is answered with respect to sensitive measuring techniques for phase, wavelength, and polarization. In principle, the fast shift of fringes can be used to speed up the switching time of a liquid crystal cell, since small changes of a phase difference (a voltage) can be translated into large polarization changes, but only at the cost of light intensity. The physical reason for this is the necessity to compensate the main polarization components of two light beams by destructive interference to be able to observe the small constructively interfering orthogonal components. The latter are only dominant in a small region where destructive interference is total and only in this region is the nonlinear effect observed.

The strong overall intensity changes of the fringe pattern which describes Pancharatnam's phase counterbalance the nonlinear phase shift of the fringes in certain orientation regions of the rotating analyzer. In spite of the fast shift of the fringes, no higher frequency components appear in the intensity spectrum. The only frequency component has double the rotation frequency of the analyzer P. This was the initial question of this study: it offended a scientist's common sense that a rotating analyzer could introduce frequency components in a linear optical interference experiment that are much higher (or lower) than its own rotation frequency.

We described a simple formalism on the Poincaré sphere to calculate the nonrelativistic development of polarized light in birefringent rotating plates and rotating analyzers and compiled the results in descriptive diagrams.

ACKNOWLEDGMENTS

The authors wish to thank Dr. Susanne Klein for her substantial help. This study was undertaken in connection with the COST 241 action.

[1] S. Pancharatnam, Proc.-Indian Acad. Sci., Sect. A **44**, 247 (1956).
[2] M. Martinelli and P. Vavasorri, Opt. Commun. **80**, 166 (1990).
[3] J. Brendel, W. Dultz, and W. Martienssen, Phys. Rev. A **52**, 2551 (1995).
[4] H. Schmitzer, S. Klein, and W. Dultz, Physica B **175**, 148 (1991).
[5] H. Schmitzer, S. Klein, and W. Dultz, Proc. SPIE **1995**, 763 (1993).

[6] B. Hils, L. Beresnev, and W. Dultz, Interferometer, Patent DE 19720246.2-52 (1997).
[7] R. Bhandari, Phys. Rep. **281**, 1 (1997).
[8] R. Ramaseshan and R. Nityananda, Curr. Sci. India **55**, 1225 (1986).
[9] M. Berry, J. Mod. Opt. **34**, 1401 (1987).
[10] For the use of the notation ''geometric'' or ''topological'' phase, see A. Mortafazadeh, Phys. Rev. A **55**, 4640 (1997).
[11] M. Berry, Proc. R. Soc. London, Ser. A **392**, 45 (1984).
[12] R. Bhandari, Phys. Lett. A **180**, 21 (1993).
[13] H. Schmitzer, S. Klein, and W. Dultz, Phys. Rev. Lett. **71**, 1530 (1993).
[14] V. Bagini, F. Gori, M. Santarsiero, F. Frezza, G. Schettini, and G. Spagnolo, Eur. J. Phys. **15**, 71 (1994). Note that this reference uses the ''nontraditional view'' of circular polarized light: R L.
[15] R. Ramachandran and S. Ramaseshan, *Crystal Optics*, edited by S. Flügge, Handbuch der Physik Vol. XXV/1 (Springer, Berlin, 1961).
[16] This formula was derived by Dr. Susanne Klein.
[17] W. Vogel and D. G. Welsch, *Lectures on Quantum Optics* (Akademie, Berlin, 1994), p. 143.